Universiteit
Leiden
The Netherlands

MAS NMR study of the photoreceptor phytochrome

Rohmer, T.

Citation
Rohmer, T. (2009, October 13). *MAS NMR study of the photoreceptor phytochrome*. Retrieved from https://hdl.handle.net/1887/14203

Version:	Corrected Publisher's Version
License:	Licence agreement concerning inclusion of doctoral thesis in the Institutional Repository of the University of Leiden
Downloaded from:	https://hdl.handle.net/1887/14203

Note: To cite this publication please use the final published version (if applicable).

Chapter 4

The Pfr → Pr photoconversion process

4.1 Introduction

The parent states of phytochrome, Pr and Pfr, have been studied in **Chapter 3**. It has been shown that the forward Pr → Pfr phototransformation is characterized by the formation of a strong hydrogen-bonding interaction on the ring ***D*** carbonyl and an increase in length and strength of the conjugation of the π-system.

At both Pr → Pfr and Pfr → Pr phototransformations, intermediate states can be distinguished [39, 43, 96]. Their structural characterization may allow for detailed insight into the mechanism of the phototriggered processes. The photochromic photocycle of various phytochromes (Fig. 1.5) has been studied by absorption and vibrational spectroscopy. For the Pr → Pfr conversion, absorption spectroscopy has identified up to three intermediates, called Lumi-R, Meta-R_a, and Meta-R_c [112–114]. For the Pfr → Pr back-reaction, two intermediates (Lumi-F and Meta-F) have been observed [113], for a recent overview on the time-resolved spectroscopy of phytochrome see [115]. These intermediates have been studied by infrared and Raman spectroscopy on various organisms [27, 30, 39, 40, 42, 43, 89, 116]. These studies suggest that Lumi-R and Meta-R are structurally different from each other as well as from Pr and Pfr, however, early studies propose that the absorption maxima of Lumi-R and Lumi-F are similar to Pr (673 and 660 nm, respectively) [113]. It should

be noted that most conversion studies have been performed in a temperature-regulated manner, allowing to trap the first intermediate at very low temperature and generating stepwise the following intermediates by gentle increase of the temperature. Thus, the given absorption maxima can deviate from such obtained at ambient temperatures by time-resolved spectroscopy.

On the other hand, much less is known about the back-reaction, which is believed to occur essentially in a single step, directly after the photoexcitation, followed by only minor relaxation steps re-arranging the cofactor-protein interactions [43, 106]. In any case, forward- and back-reactions are very different processes and not simply mirror-symmetric transformations. The intermediates of the back-reaction, Lumi-F and Meta-F, have been shown in the CphA phytochrome from the cyanobacterium *Calothrix* sp. PCC 7601 to absorb at 635 and 640 nm, respectively [116]. The strong blue-shift in the initial phototransformation step is not fully understood. In addition, the specific characteristics of the Lumi-F and Meta-F intermediates have not yet been described.

In **Chapter 3**, the two parent states of the phytochrome system Pr and Pfr have been studied by ^{1}H , ^{13}C and ^{15}N CP/MAS NMR. In this chapter, the intermediates of the back-reaction of phytochrome Cph1, Lumi-F and Meta-F, are investigated by ^{1}H, ^{13}C and ^{15}N CP/MAS NMR. Uniformly ^{13}C and ^{15}N as well as selectively ^{15}N labeled samples are used for signal assignment. The intermediates were trapped directly in the magnet with illumination at low temperature. Light-triggered low-temperature MAS NMR investigations of intermediates have recently also been presented on rhodopsin [117], bacteriorhodopsin [118] and adenylyl transfer reaction of T4 DNA ligase [119].

4.2 Results

4.2.1 Conformational changes of the cofactor carbon atoms

The 2D ^{13}C-^{13}C MAS DARR spectra of the Lumi-F and Meta-F intermediates are show in Figures 4.1 and 4.2, respectively. From these data, almost complete sets of ^{13}C assignments have been obtained for both intermediate states (Table 4.1). In the 2D spectra of both Lumi-F and Meta-F, the resonances of the aromatic carbons have been assigned through their correlation with the methyl, ethyl or propionic substituents. The carbon atoms C9 and

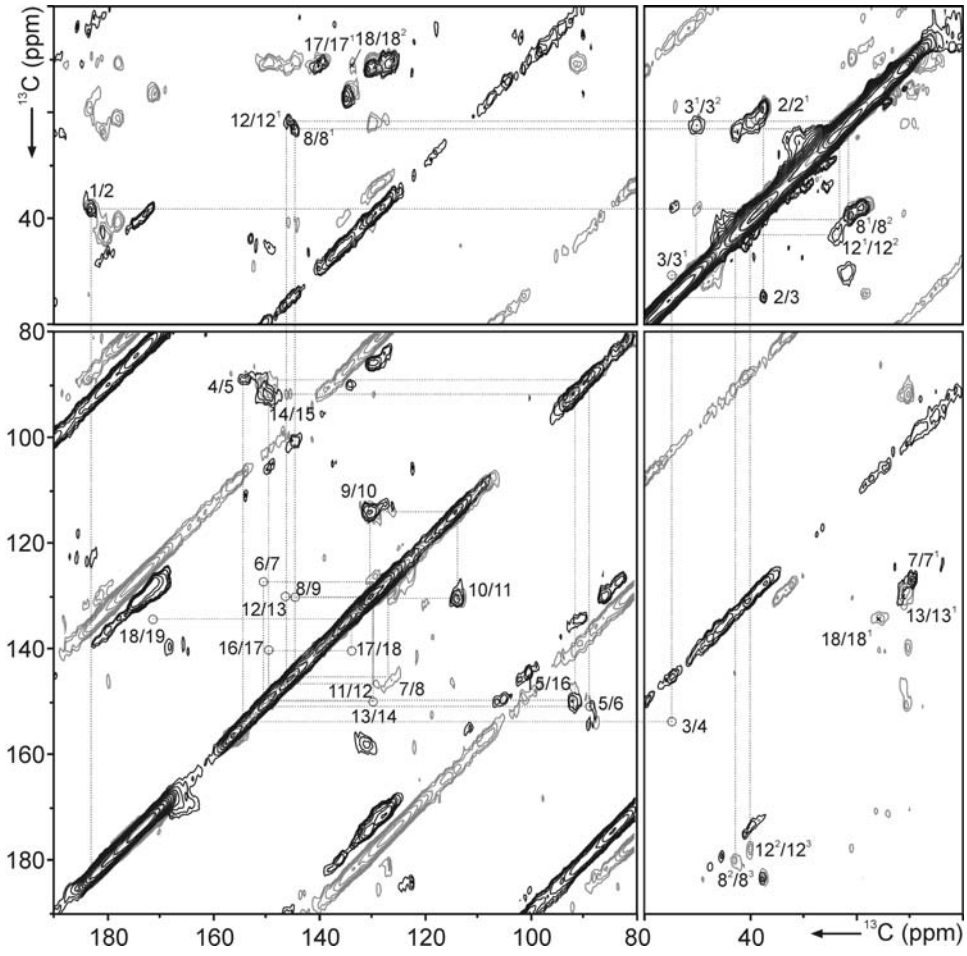

Figure 4.1: Contour plot of the 2D ^{13}C-^{13}C DARR NMR spectra of u-[^{13}C,^{15}N]-PCB-Cph1Δ2 in the Lumi-F state using proton mixing times of 5 and 50 ms (black and grey, respectively). Spectra recorded at 173 K and spinning frequencies of 9 and 10 kHz.

C11 as well as C14 and C16 overlap in both intermediate states (Table 4.1).

The changes of chemical shifts during the three transitions of the back-reaction (Pfr → Lumi-F, Lumi-F → Meta-F, Meta-F → Pr) for selected carbons is shown in Figure 4.3. The general features are: (*i*) The major changes occur at the carbons between C13 and C19, and (*ii*) the transformations during the two first transitions are significantly larger than during the third transition. The large chemical shift changes during the second transition are

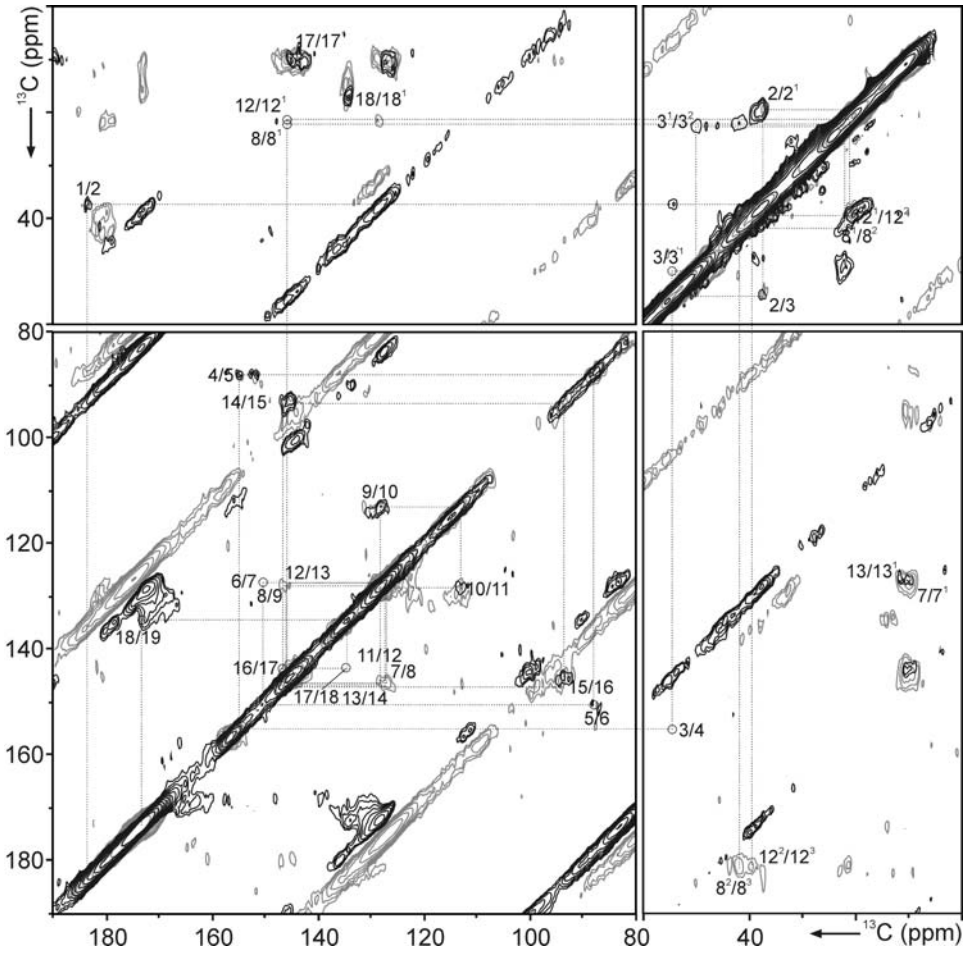

Figure 4.2: Contour plot of the 2D ^{13}C-^{13}C DARR NMR spectra of u-[^{13}C,^{15}N]-PCB-Cph1Δ2 in the Meta-F state using proton mixing times of 5 and 50 ms (black and grey, respectively). Spectra recorded at 203 K and spinning frequencies of 9 and 10 kHz.

unexpected. Hence, the transition from Lumi-F to Meta-F appears to be more than a simple relaxation process. Spatial details can be better recognized in Figure 4.4. At the C19 carbonyl group, the changes occur during the first two transitions to roughly the same extent. In **Chapter 3**, it has been concluded that the Pfr state is characterized by hydrogen-bonding interactions stronger than in Pr. It appears that the weakening of these interactions occurs in two steps. During the first transition, a significant change occurs selectively at

Position	Pfr	Lumi-F	Meta-F	Pr
C1	182.8	183.2	183.6	182.5
$C1^a$	—	—	—	184.0
C2	37.2	37.3	37.1	37.1
$C2^a$	—	—	—	38.1
$C2^1$	18.5	18.6	18.6	17.5
C3	54.3	54.3	54.0	53.4
$C3^1$	50.0	50.0	49.2	47.6
$C3^2$	21.6	21.9	22.0	21.8
C4	154.0	n.d.	154.0	153.9
C5	88.5	88.5	87.5	87.1
C6	148.8	n.d.	n.d.	149.1
C7	126.1	126.7	126.1	126.1
$C7^1$	9.3	9.5	9.3	9.2
C8	143.6	144.6	145.5	144.5
$C8^1$	23.1	23.4	22.0	22.5
$C8^{1a}$	—	—	—	21.5
$C8^2$	41.7	42.6	42.8	43.1
$C8^{2a}$	—	—	—	41.1
$C8^3$	180.5	180.8	180.6	180.5
$C8^{3a}$	—	—	—	179.7
C9	131.0	130.1	128.1	127.7
C10	112.3	113.8	112.9	112.7
C11	131.0	130.1	128.1	127.7
C12	145.8	145.7	145.5	145.5
$C12^1$	20.6	21.0	21.0	21.1
$C12^2$	38.3	40.0	38.3	37.5
$C12^3$	175.2	178.2	179.1	179.5
C13	130.6	129.9	126.2	126.3
$C13^1$	11.9	11.8	11.5	11.7
C14	151.5	149.5	145.4	145.7
C15	91.7	91.9	93.2	93.5
C16	151.1	149.5	145.4	145.7
C17	137.7	139.8	143.2	142.2
$C17^1$	10.1	10.1	10.2	9.8
C18	140.4	134.4	134.2	134.3
$C18^1$	15.6	15.6	16.1	16.1
$C18^2$	13.3	n.d.	n.d.	13.3
C19	168.4	171.8	172.7	172.8

Table 4.1: ^{13}C chemical shifts obtained for Cph1Δ2 containing an u-[^{13}C,^{15}N]-PCB chromophore.

position C18, and also a change of the chemical shift of the $C12^3$ carboxylic group of ring ***C*** occurs already during this first transformation. C18 shows no further changes, whereas during the second transition, in addition to a large C13 change, both ring carbon neighbors of the C10 and C15 bridges are affected. It appears that the dark single bond transformation following the

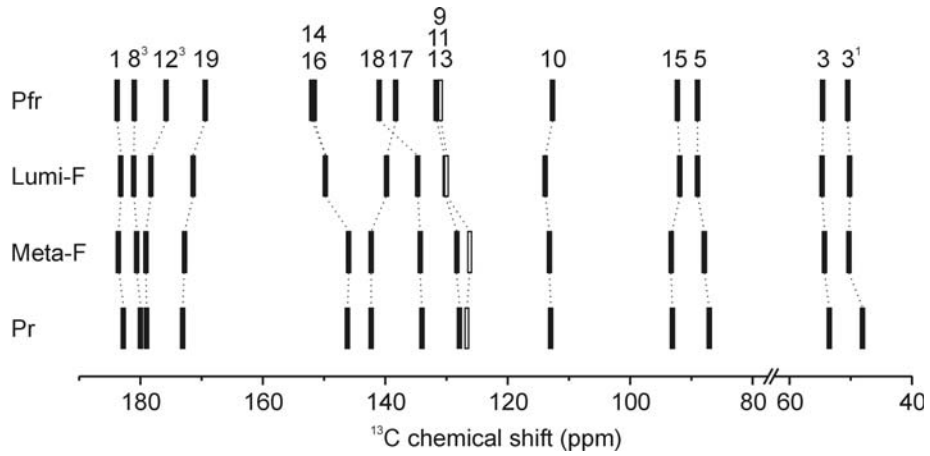

Figure 4.3: ^{13}C chemical shifts for selected carbon atoms during the Pfr → Pr back-reaction. For seek of clarity, the ^{13}C resonance of C13 is indicated by an open rectangle.

light-induced double bond isomerization affects the electronic structure even stronger. The unit formed by rings ***A*** and ***B*** shows less extensive effects, those that are seen affecting the C3^1 thioether linkage to Cys-259. In fact, perhaps the biggest surprise is that only very weak shifts were found to be associated with C15. Also interesting is that the ring ***B*** propionic carbons show only minimal changes.

4.2.2 Assignment of the nitrogen atoms

The 1D ^{15}N spectra of ^{15}N21-PCB-Cph1Δ2 labeled phytochrome in the Pr, Pfr, and the intermediate states are presented in Figure 4.5, Column A. The N21 nitrogen atom exhibits a ^{15}N chemical shift at around 158 ppm and appears to be only weakly affected during the Pfr to Pr back-reaction. This is in line with the weak changes along ring ***A*** during the Pfr → Pr conversion deduced from the ^{13}C chemical shifts. The equivalent ^{15}N CP/MAS spectra of the u-^{15}N-PCB-Cph1Δ2 are shown in Figure 4.5, Column B. The deconvolutions of the Lumi-F and Meta-F spectra using Voigt functions are shown in Appendix C, Figure C.1. In the Lumi-F states, two ^{15}N resonances overlap at 157.9 ppm and two other signals are observed at 146.0 and 136.5 ppm. The Meta-F intermediate presents four peaks at 161.1, 156.0, 144.8 and 127.1 ppm.

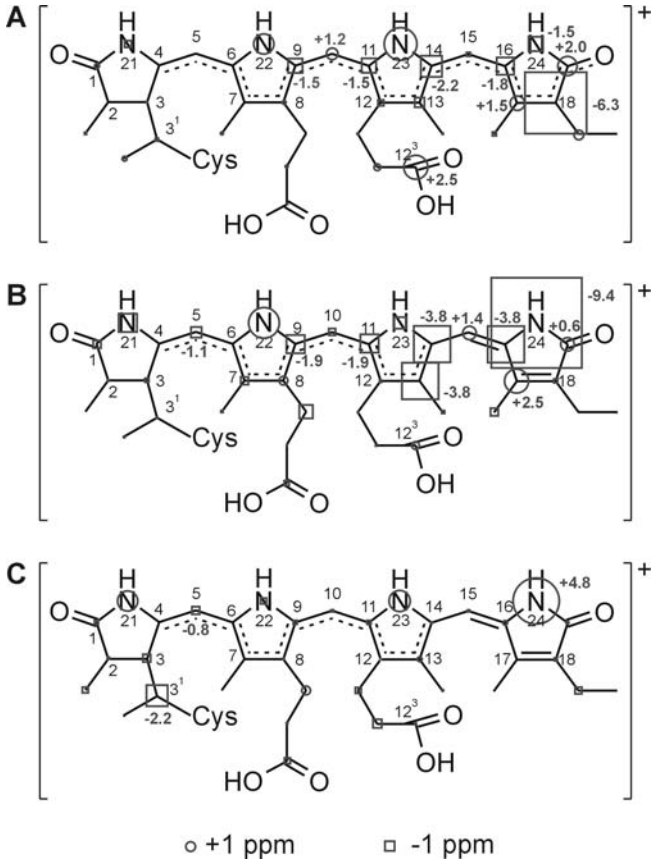

Figure 4.4: Change in ^{13}C and ^{15}N chemical shift of the u-[^{13}C,^{15}N]-PCB chromophore in Cph1Δ2 during the Pfr → Lumi-F (**A**), Lumi-F → Meta-F (**B**) and Meta-F → Pr (**C**) transitions. For each transition, the starting state is taken as reference and the size of the circles and squares refers to the difference in ^{13}C and ^{15}N chemical shifts in the next state.

One of the overlapping peaks at 157.9 ppm in the Lumi-F state is attributed to N21. The signal at 156.0 ppm in the Meta-F state is tentatively assigned to the ring ***A*** nitrogen (Table 4.2). It has been proposed in **Chapter 3** that the ring ***D*** nitrogen resonance occurs at 131.9 and 138.0 ppm in the Pr and Pfr state. In analogy, it can be assumed that the signals at 136.5 and 127.1 ppm arise from N24 in the Lumi-F and Meta-F intermediates, respectively. Similarly, the signals at 146.0 and 144.8 are tentatively assigned to N23 in Lumi-F and Meta-F, respectively. Finally, the two remaining signals at 157.9 and 161.1 ppm in Lumi-F and Meta-F originate from N22.

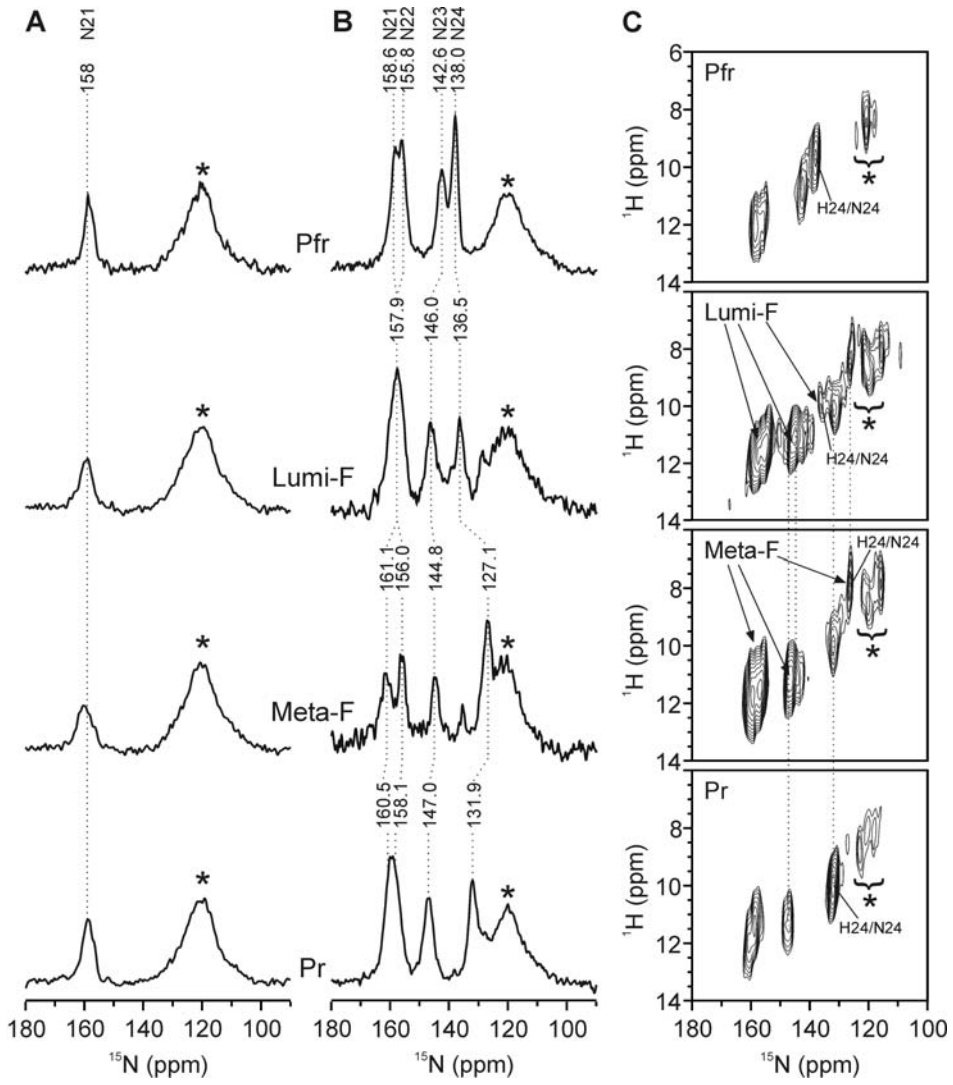

Figure 4.5: 1D ^{15}N spectra of ^{15}N21-PCB-Cph1Δ2 (column **A**) and u-^{15}N-PCB-Cph1Δ2 (column **B**) in the Pfr, Lumi-F, Meta-F and Pr states recorded at 17.6 T with a spinning frequency of 8 kHz and at 243 K, 173 K, 203 K, and 243 K, respectively. 2D ^{1}H-^{15}N FSLG heteronuclear correlation spectra of Pfr, Lumi-F, Meta-F, and Pr (Column **C**). The spectra of the intermediates were obtained from a Pfr:Pr (1:1) mixture.

4.2.3 Changes of the nitrogen atoms

The Pfr → Lumi-F transition causes a shift of the N22 and N23 responses by +2.1 and -3.4 ppm, respectively (Fig. 4.4), while changes of the other ni-

Position	Pfr	Lumi-F	Meta-F	Pr
N21	158.6	157.9	156.0	158.1
N22	155.8	157.9	161.1	160.5
N23	142.6	146.0	144.8	147.0
N24	138.0	136.5	127.1	131.9

Table 4.2: Tentative ^{15}N chemical shift assignment of u-[^{13}C,^{15}N]-PCB chromophore in Cph1Δ2 during the Pfr → Pr conversion.

trogen atoms are smaller (-0.7 and -1.5 ppm for N21 and N24, respectively). Also the proton chemical shifts (Fig. 4.5, column C) do not undergo any significant change during this step. The Lumi-F → Meta-F transition shows a strong change at N24, which shifts 9.4 ppm downfield. Interestingly, this change is linked to an upfield shift of the H24 pyrrole proton from ∼10 to ∼8 ppm (Fig. 4.5, column C), suggesting a modification of hydrogen-bonding in the Meta-F intermediate state. In addition, also the signal assigned to the ring ***B*** nitrogen shifts from 157.9 to 161.1 ppm, however, no significant proton shift can be observed. The Meta-F → Pr transition is also associated with significant chemical shift changes of the ring ***D*** nitrogen and the pyrrole proton, indicating that the a hydrogen-bonding interaction is restored at this position. The nitrogen atom N21 and N23 are also affected during this transition (+2.1 and +2.2 ppm, respectively).

4.3 Discussion

4.3.1 The Pfr → Lumi-F transition

It has been proposed that the chromophore in the Pfr state is in a conformationally strained state [43, 104, 120], requiring a strong fixation of the ring ***D*** in the pocket. To this end, a strong hydrogen-bond of the ring ***D*** carbonyl has been proposed, leading to enhanced conjugation from ring ***A*** to ring ***D*** that increases the stiffness of the cofactor [14, 120]. On the other hand, the significant chemical shift change at C18 is specifically associated with the Pfr to lumi-F primary photoreaction. This might result from a mechanical interaction of the C18 ethyl group associated with the strained cofactor state. Indeed, the thermal stability of oat phytochrome A in the Pfr state is improved when the size of the C18 sidechain group is increased [121]. In a recent X-ray structure on the Pfr-like state of *Pseudomonas aeruginosa* PaBphP [55], however, no residues close to the ethyl group are observed. Similarly, the Pr

structure of Cph1 [53] does not provide any clue to a possible interaction. This effect may be related to the changes on the electronic structure directly induced by the photoisomarization and the change of hydrogen-bonding interaction at the C19 carbonyl [120, 122]. Hence, it appears that the extended conjugation is already broken in the Lumi-F state, as demonstrated by its strongly blue-shifted absorption [116].

The ring ***D*** nitrogen is protonated and hydrogen-bonded in the Pfr state (Fig. 4.5, Column C). Since the changes in the ^{15}N shift of N24 as well as at the ^{1}H resonance of its bound proton are small, it can be assumed that the hydrogen-bonding interaction remains even after the photoisomerization, implying that the cofactor is not yet fully relaxed in the Lumi-F state. On the other hand, the hydrogen-bond at the C19 carbonyl weakens during the initial Pfr → Lumi-F transition. The fact that the hydrogen-bond of the ring ***D*** nitrogen remains almost unchanged in Lumi-F suggests that the hydrogen-bonding partner is very strong. From the crystal structure of Cph1Δ2 in the Pr state, the hydrogen-bonding partner has been shown to be a water molecule [53]. Comparing the ^{15}N chemical shifts of Pfr, Pr and the intermediate Meta-F, where this hydrogen-bond is broken, it is further concluded that the hydrogen-bonding partner in Pfr is stronger than water. It has been shown by mutational studies that Asp-207 is crucial for the formation of the Pfr state [19, 98]. As suggested by the X-ray structure of the Pfr-like state, the carboxylic group of the side-chain of Asp-207 could indeed be the strong hydrogen-bonding partner of N24 in the Pfr state.

The maintenance of the hydrogen-bond at N24 is difficult to reconcile with a full 180° rotation of ring ***D*** during the photoisomerization. Studying a phytochrome model compound in solution, Stanek and Grubmayr [103] have shown that the isomerization of the C15=C16 double bond affects strongly the ^{13}C chemical shift of the C15 carbon (7 ppm upshift upon E/Z isomerization). In solution, such an E/Z isomerization generates the flip of the ring ***D*** by about 180°. For the Pfr → Lumi-F transition, however, only a weak effect is observed at the C15, although it cannot be ruled out that other effects might mask the expected large change at this position. In any case, the first trapped photochemical event involves something different from a classical full 180° rotation of ring ***D*** associated with a complete E/Z isomerization as observed in solution.

Interestingly, the protein pocket around the C12^3 carboxylic group of the

ring ***C*** propionic side-chain appears to be already re-arranged in the Lumi-F intermediate. In particular the position of His-290 may be re-arranged into its Pr position and may already interact with the ring ***D*** carbonyl group.

4.3.2 The Lumi-F → Meta-F transition

The Pfr → Lumi-F transition is characterized by the photochemical *E*-to-*Z* C15=C16 double bond isomerization, while the Lumi-F → Meta-F transition is related to thermal processes. This transition is characterized by the full release of ring ***D*** from its tensed state as indicated by two significant changes: (*i*) the loss of hydrogen-bond interaction at the ring ***D*** nitrogen and (*ii*) a second stronger change of the C10 and C15 methine bridges. It appears that the chromophore is fully relaxed in Meta-F, while in Lumi-F the hydrogen bridge at the ring ***D*** nitrogen is still preventing a full rotation of the ring. It is surprising that during the Lumi-F → Meta-F transition the changes around methine bridges C10 and C15 are stronger than in the Pfr → Lumi-F transition.

4.3.3 The Meta-F → Pr transition

As the chromophore has already been relaxed in the Meta-F state, the changes along the conjugated system are very minor with respect to the ^{13}C chemical shift. Interestingly, the main effects occur at C3^1, the cofactor-matrix link, and at N24 which is re-bound *via* a hydrogen-bonding interaction to a water molecule as seen in the X-ray structure of the Pr state [53]. Additional minor changes indicate an overall re-arrangement of the chromophore-protein interactions, potentially involving – not observable – movements of the protein environment.

4.3.4 Model for the back-reaction

The ^{1}H, ^{15}N and ^{13}C CP/MAS NMR data indicate that the strained chromophore in Pfr is associated with four important effects (Fig. 4.5A): (*i*) The increased conjugation changing C–C single bonds to partially higher bond orders and double bonds to partially lower bond orders, (*ii*) the strong hydrogen-bond of the C19 carbonyl to Tyr-263, as shown in the crystal structure of PaBphP in its Pfr-like ground state, (*iii*) the strong hydrogen-bonding of

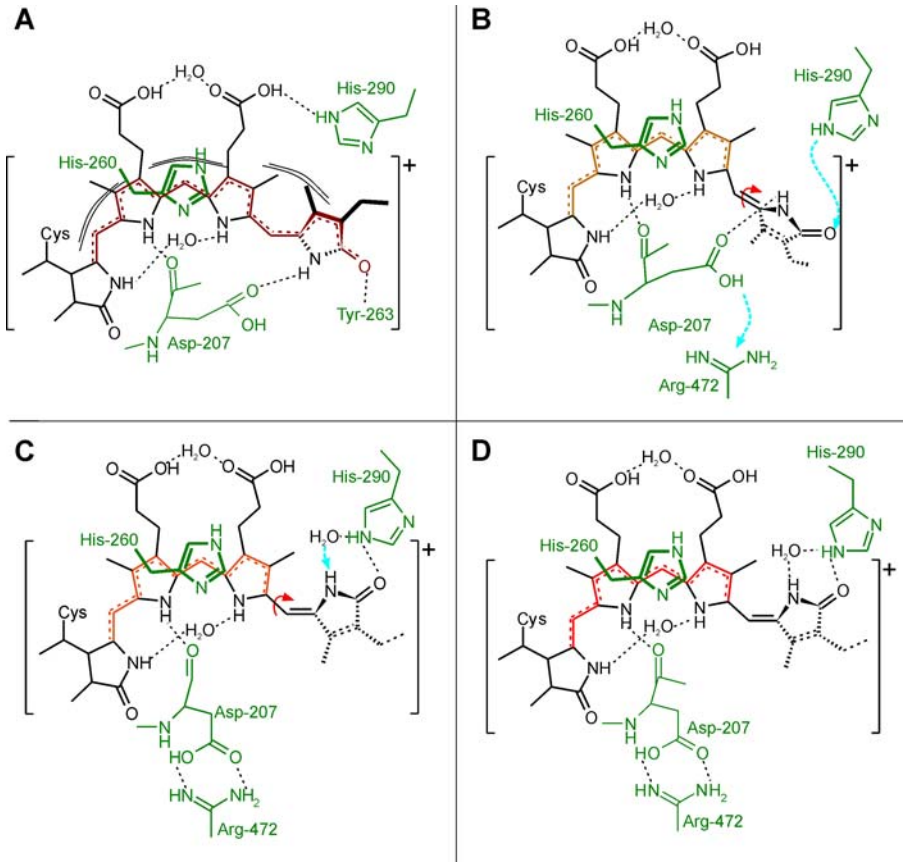

Figure 4.6: Proposed structures and conformational changes of the tetrapyrrole chromophore and its binding pocket in the Pfr (**A**), Lumi-F (**B**), Meta-F (**C**) and Pr (**D**) states. The conjugated system is shown in dark red (Pfr), orange-red (Lumi-F, Meta-F) and red (Pr). The rotations around the double and single bond of the C15 methine bridge are shown by solid arrows. The dashed arrows indicate potential paths of signal transmission within the chromophore binding pocket. Protein residues are indicated in green.

ring ***D*** nitrogen, presumably to Asp-207 and (*iv*) a potential mechanical blocking mechanism associated with the C18 ethyl group would be an obvious hypothesis, however the X-ray structural data do not reveal any interaction in this region. In addition, the X-ray structure of *Pseudomonas aeruginosa* PaBphP in the Pfr state shows that the His-290 homolog provides an anchor for the C12[3] carboxylic group of the chromophore.

The Lumi-F state (Fig. 4.5B) is characterized by (*i*) a shorter and weaker conjugation system, (*ii*) a partial relaxation of the cofactor due to incomplete rotation of the ring ***D*** caused by the release of the C19 carbonyl hydrogen-bonding interaction, as well as (*iii*) a matrix re-arrangement around the carboxylic group of the ring ***C*** propionic side-chain.

The Meta-F state (Fig. 4.5C) is described by (*i*) the full relaxation of the chromophore after breaking the hydrogen-bond of the ring ***D*** nitrogen to the carboxylic group of the side-chain of Asp-207 allowing to complete the rotation of the C15 single bond and (*ii*) the formation of a new hydrogen-bond between C19 carbonyl and His-290.

In the Pr state (Fig. 4.5D), in which the cofactor is fully relaxed and hydrogen-bonded, (*i*) a new hydrogen-bond at ring ***D*** nitrogen is formed by a water molecule, and (*ii*) protein relaxations have occurred.

The CP/MAS NMR data show that the back-reaction includes two intermediates which can be structurally clearly distinguished, and which adopt a conformation and electronic arrangement different than the two parent states Pr and Pfr.

4.3.5 Model for signal transduction

The data presented here describe the changes of the Cph1 chromophore from Pfr to the Pr ground state. Thus, the observed changes of the chromophore and the protein during the transition from Pfr to Lumi-F, followed by the Meta-F to Pr state reflect changes that are connected to both photoconversion and signal transduction.

The data shown in this chapter reveal that the Pfr → Pr photoconversion is associated with changes to the $C12^3$ carboxylic group of ring ***C*** and the entire ring ***D*** *via* its two hydrogen-bonds. Thus, the state change is linked to separate chromophore-protein interactions at opposite sides of the chromophore, *i.e.*, at $C12^3$ and the entire ring ***D***. The highly conserved His-290 – bound to the C19 carbonyl in Pr [53] and to the $C12^3$ carboxylic group in the Pfr-like ground state of PaBph3 [55] – faces inwards from a β-sheet at the surface of the molecule. Although the imidazole of its equally well conserved neighbor, His-291, is exposed to the solvent in both X-ray structures, a signaling mechanism is not obvious. Similarly, from the $C12^3$ no molecular signal pathway is immediately apparent although the interactions implied by the X-ray structures are very different in the Pr and Pfr states.

Conversely, no obvious changes are associated with the ring ***B*** propionic side-chain, although a salt bridge partner-swap between Arg-222 and Arg-254 is implied by the crystal structures and would accord with a similar possible re-arrangement in the oxygen-sensing domain of *Bradyrhizobium japonicum* FixL [53, 123].

On the other hand, the Asp-207/Arg-472 salt bridge connecting the PHY domain tongue to the chromophore region [53] is replaced by additional interactions with N24 and probably Ser-474 in the Pfr-like PaBph3 structure [55]. All these residues are highly conserved and are thus likely to fulfill essential functions in all phytochromes, Asp-207 being particularly important for stabilizing the Pfr state [19, 98]. The present data confirm that the hydrogen-bonding interaction between N24 and Asp-207 is associated with a break of the salt bridge between Asp-207 and Arg-472 in the Pfr state as implied by the PaBph3 structure [55]. It has to be pointed out, however, that the latter is not likely to be an entirely reliable model for the Pfr state in Cph1 and other plant-type phytochromes.

The tongue region comprises a most unusual hairpin structure inserted into the otherwise GAF/PAS-like PHY domain, making intimate contact with the extreme N-terminus of the molecule, itself unusual in forming a knot by passing through a loop in the GAF domain itself. The data presented in this chapter indicate that the Asp-207/Arg-472 association is likely to couple light-induced changes in chromophore geometry to the tongue and probably the N-terminus, thus it can be proposed that its disruption is central to photochromicity and/or the intramolecular signal transduction pathway. In the Lumi-F state, the ring ***D*** nitrogen is still hydrogen-bonded to Asp-207, while this interaction is disrupted in the Meta-F state, suggesting that the main re-arrangements of the protein are triggered at this step.

4.4 Materials and Methods

4.4.1 Sample preparation for MAS NMR spectroscopy

The u-[^{13}C,^{15}N]-PCB was prepared following the method presented in section 3.4.1. The chemical synthesis of the ^{15}N21-PCB sample has been carried out by Dr. C. Bongards (Max-Planck-Institut, Mülheim an der Ruhr, Germany). The synthesis is briefly described in the Appendix C.

4.4.2 MAS NMR spectroscopy

About 15 mg of u-[^{13}C,^{15}N]-PCB-Cph1Δ2 protein in the Pfr state were placed in a 4-mm zirconia rotor. The Lumi-F and Meta-F intermediate states were thermally trapped in the magnet by illumination through a far-red cut-off filter ($\lambda_{max} = 730$ nm) at 173 K and 203 K, respectively. The illumination setup used has been specially designed for a Bruker MAS probe [124]. 2D ^{13}C-^{13}C DARR experiments were performed at a field of 17.6 T on an Avance-WB750 spectrometer, equipped with a 4-mm triple resonance CP/MAS probe (Bruker, Karlsruhe, Germany). The ^{13}C-^{1}H dipolar interaction has been recovered by CW irradiation on ^{1}H RF intensity to satisfy the n = 1 condition. ^{1}H $\pi/2$- and ^{13}C π-pulse lengths were set at 3.1 and 5 μs, respectively. The ^{1}H power was ramped 80-100% during CP. Mixing times of 5 and 50 ms were used. ^{1}H CW decoupling was about 80 kHz during the proton mixing and about 43 kHz TPPM during acquisition. The DARR spectra were recorded with about 1 kscans, and with 8 μs evolution in the indirect dimension, leading to experimental times of about 60 h. The data were processed with the Topspin software version 2.0 (Bruker, Karlsruhe, Germany) and subsequently analyzed using the program Sparky version 3.100 (T. D. Goddard & D. G. Kneller, University of California, San Francisco, USA).

1D ^{15}N CP/MAS spectra were recorded using an AV-750 spectrometer, equipped with 4-mm CP/MAS probe. ^{1}H-^{15}N heteronuclear experiments were performed at the Avance-WB750, using a frequency switched Lee-Goldburg pulse sequence [68]. The proton $\pi/2$-pulse was set to 3.1 μs and the spinning frequency was 8 kHz.